Heterogeneity of the Segmental Dynamics of Poly(dimethylsiloxane) in a Diblock Lamellar Mesophase: Dielectric Relaxation Investigations

C. Lorthioir,*,†,‡ A. Alegría,† J. Colmenero,†,‡ and B. Deloche§

Departamento de Física de Materiales, Universidad del País Vasco (UPV/EHU) y Unidad de Física de Materiales Centro Mixto (CSIC-UPV/EHU), Facultad de Química, Apartado 1072, 20080 San Sebastián, Spain; Fundación Donostia International Physics Center, Paseo Manuel de Lardizabal 4, 20018 San Sebastián, Spain; and Laboratoire de Physique des Solides (CNRS-UMR 8502), Université Paris-Sud, 91405 Orsay, France

Received May 19, 2004; Revised Manuscript Received July 27, 2004

ABSTRACT: The segmental dynamics of amorphous poly(dimethylsiloxane) (PDMS) in a lamellar poly(styrene)−poly(dimethylsiloxane) diblock (PS−PDMS) is investigated by means of broadband dielectric spectroscopy. Because of the absence of normal mode in PDMS, we have been able to analyze the low-frequency side of the α-relaxation in detail. The characteristic time of the segmental dynamics is found to be significantly higher than that in a PDMS homopolymer. In addition, the dielectric loss peak displays a pronounced broadening in the low-frequency side as compared with that observed in pure PDMS. We showed that the $\epsilon''(\omega)$ curves could be well described assuming two types of PDMS segments depicting qualitatively distinct segmental dynamics. In one case, the dielectric response is similar to that one of the amorphous constrained phase in a cold-crystallized PDMS homopolymer. For the other segments, the dielectric behavior appears close to that one of an amorphous PDMS homopolymer. However, some differences remain indicating a significant gradient of mobility within this second type of PDMS segments. We explain all these findings by considering a simple picture of the PDMS segments in the PS−PDMS lamellar mesophase.

1. Introduction

The chain dynamics within microphase-separated block copolymers has been widely studied at different length and time scales: diffusive motions of the copolymer chains in the various well-defined microstructures that block copolymers can exhibit (lamellae,[1,2] cylinders,[3] or spheres,[4] for instance), reorientational motions of the different blocks,[5−10] and at a shorter length scale the segmental motions.[5,7−12] In particular, broadband dielectric relaxation spectroscopy has proved to be an efficient way to probe the fluctuations of the chain end-to-end vector for each block as well as the segmental motions.[13] The segmental motions along the chain backbone induce fluctuations of the monomeric dipolar moments and give rise to the dielectric α-relaxation. In addition, for type A polymers, the monomer dipole components on the chain contour direction do not cancel, giving rise to a resulting nonzero dipole moment. The time fluctuations of this dipole moment are related to the so-called dielectric normal mode, sensitive to the reorientational motions of the block end-to-end vector. Studying ordered block copolymers made of at least one type A polymer is very instructive since it allows to probe the chain dynamics of the corresponding block at two different length scales (a few nanometers for the segmental mode and tens of nanometers for the normal mode) and to make some comparisons with the dynamics of homopolymer chains. For this reason, most of the block copolymers investigated up to now were based on high cis content poly(isoprene) (PI) sequences.[14] The chain and segmental dynamics within the ordered phases of PI-based block copolymers exhibiting different degrees of complexity in their structural architecture have been investigated: lamellar diblocks,[5,15] diblocks displaying 2D or 3D mesophases,[11] symmetric triblocks,[6,16,17] and star copolymers.[7] When comparing with PI homopolymers of similar molecular weight, no great change was observed on the segmental mode. By contrast, a lot of attention has been dedicated to the dielectric normal mode. Indeed, this relaxation process was found to display more dramatic variations by comparison with the pure homopolymer. Besides, the analysis of the normal mode—the dependence of the characteristic relaxation time with the chain length for instance—enables the comparison with the results predicted by theoretical models concerning chain dynamics.[18] However, the segmental mode usually overlaps with the normal mode, located at lower frequencies. Because of this overlapping, a detailed analysis of the α-process—particularly the shape of the relaxation process in the low-frequency part—is hardly possible. The dynamics in other block copolymers made of type A blocks has also been investigated using dielectric spectroscopy, such as poly(oxybutylene) in poly(oxybutylene)−poly(oxyethylene) diblocks for instance,[8] and the same general trends mentioned above are also observed for both normal and segmental modes.

In the present work, we have considered a poly(styrene)−poly(dimethylsiloxane) (PS−PDMS) diblock. Because of the difference in the dielectric strength between PS and PDMS, the dielectric response is governed by the dynamics of the PDMS blocks. PDMS is well-known to be a type B polymer so that only the segmental motions (α-process) are observed. Last, because of its simple molecular structure, no secondary relaxation process overlaps with the segmental mode. For all these reasons, PS−PDMS diblocks are well-suited systems to capture the whole frequency depend-

† Universidad del País Vasco.
‡ Fundación Donostia International Physics Center.
§ Université Paris-Sud.
* Corresponding author: Tel +33 1 49 78 12 28; Fax +33 1 49 78 12 08; e-mail lorthioir@glvt-cnrs.fr.

10.1021/ma049011t CCC: $27.50
Published on Web 09/11/2004

Table 1. Molecular Characteristics of the Systems Investigated in This Work

sample	M_w[a]	I_w[b]	M_w(PS)[a]	I_w(PS)[b]	ϕ_{PDMS}[c]
PS−PDMS(D)	21600	1.04	10000	1.01	0.53
PDMS(H)	14881	1.06			1

[a] Weight-average molecular weight (g mol^{-1}). [b] Polydispersity index. [c] Volume fraction of PDMS.

ence of the α-relaxation and thus to get a detailed analysis of the segmental motions within the ordered mesophases of block copolymers.

In the PS−PDMS diblocks, the PDMS chain extremities are tethered to the PS microdomains. Because of this anchoring, the relaxation time characterizing the reorientational motions of the whole PDMS blocks is 4 times higher than in the pure homopolymer.[5,19] At a shorter length scale, the effect of the PDMS chain anchorage on the segmental dynamics has never been described. Such a description is important to understand the mechanical and viscoelastic behavior of lamellar diblocks for instance. From another point of view, in the intermediate temperature regime between the glass transition temperature T_g of the PS and the PDMS blocks, the "fluid" PDMS chains are confined by the PS microdomains: for lamellar diblocks, the PDMS chains undergo a 1D confinement, the confining distance between the PS "solid walls" ranging from a few nanometers to about 10 nm. Such a confinement can affect the chain relaxation (normal mode), but also the segmental dynamics.[19−22] In the case of PDMS, the question of the chain confinement effects on the α-process of amorphous chains was recently addressed for PDMS oligomers confined within nanopores[23] and for PDMS chains within grafted thin films.[24] In some cases, even secondary relaxation processes, though localized to a few chemical bonds, have been found to be modified by the confinement of the polymer chains.[25]

In this work, the segmental dynamics of the confined and anchored PDMS chains within the lamellar mesophase of a PS−PDMS diblock has been investigated by means of broadband dielectric spectroscopy. Because of the anchoring junctions, some segments close to the interfaces with the PS blocks are found to display a dynamical behavior similar to PDMS segments in the rigid amorphous phase (RAP) of a semicrystalline PDMS homopolymer. Other segments within the lamellae are characterized by a segmental dynamics similar to that one observed in a purely amorphous PDMS homopolymer. These segments are probably located in the center of the lamellae. However, the dynamics within the inner lamellae is not totally homogeneous, and a distribution of relaxation times ranging from the bulklike to the RAP-like values is evidenced.

2. Experimental Section

The poly(styrene)−poly(dimethylsiloxane) (PS−PDMS) diblock was synthesized starting from the anionic polymerization of styrene (in benzene, at room temperature, using *sec*-butyllithium as initiator) and then turning to the ring-opening polymerization of hexamethylcyclotrisiloxane (in a benzene/THF mixture, at room temperature). Further details concerning the synthesis can be found elsewhere.[26] For the purpose of simultaneous ^{2}H NMR investigations,[26] the PDMS sequences were perdeuterated. The PS−PDMS diblock was characterized by gel permeation chromatography (GPC), leading to the molecular parameters (weight-average molecular weight M_w, polydispersity index I_w) reported in Table 1.

PS and PDMS are two polymers strongly incompatible: using $\chi \approx 106/T$ for the temperature dependence of the Flory interaction parameter χ between PS and PDMS,[27] the product χN is estimated to be about 86 at room temperature, N being the number of monomer units in a copolymer chain. Thus, the diblock is expected to display a microphase-separated structure, which is indeed the case, as evidenced by SAXS measurements. These latter have shown a lamellar structure, with a periodicity of 22.6 nm and a thickness for the PDMS sublayers of 12.0 nm.[26]

A nonlabeled PDMS homopolymer having similar molecular characteristics than the PDMS sequence in the diblock (see Table 1) has been obtained by anionic polymerization and will be used as a reference in this work. By comparing the dielectric permittivity ϵ^* recorded on this homopolymer and on a perdeuterated one (having exactly the same chain length: number of monomer units $N = 218$), we have checked that the deuteration plays no role on the dielectric response.

Measurements of the complex dielectric permittivity $\epsilon^* = \epsilon' - i\epsilon''$ vs frequency were performed in the range 10^{-2}−10^7 Hz, using a Novocontrol high-resolution dielectric analyzer (Alpha-S analyzer). The PDMS homopolymer (low viscosity at room temperature) was inserted between two gold-plated stainless steel electrodes (diameter of 30 and 40 mm), and a separation of 100 μm between both electrodes was maintained by four small Teflon spacers. In the case of the copolymer, the diblock powder was pressed at 423 K (i.e., $T \approx T_g$(PS) + 60 K) for 5 min between two electrodes (diameter of 20 and 30 mm) and then transferred to a vacuum oven. To relax the residual constraints, the sample was kept at 423 K for more than 1 day, and then the temperature was slowly decreased to 300 K for 1 day.

The probed temperature range (147−180 K) includes temperatures for which PDMS crystallizes. To avoid this crystallization process during the cooling step, all the samples studied herein were quenched in liquid nitrogen. The cooling rate (≈110 K min^{-1}) enables to avoid crystallization of the PDMS chains.[28,29] Then, the sample cell was set in a cryostat, and its temperature was controlled via a nitrogen gas jet heating system coupled with a Novocontrol Quatro controller. The accuracy on the temperature value was better than 0.1 K within the temperature range of interest.

3. Results

The aim of this work is to perform a detailed study of the segmental relaxation within the PDMS sublayers of a PS−PDMS diblock lamellar mesophase. A precise analysis requires a fine knowledge of the dielectric behavior of the corresponding PDMS homopolymer. Thus, in the following, we will first present results obtained on a PDMS homopolymer characterized by a chain length similar to that of the PDMS sequence in the diblock.

3.1. PDMS Homopolymer. Figure 1a shows the dielectric loss $\epsilon''(\omega)$ recorded isothermally on the PDMS homopolymer—primarily quenched in liquid nitrogen—by increasing temperature in steps from 147 to 180 K. Below 155 K, a single relaxation process is observed within the probed spectral window: it is related to the segmental mobility within amorphous PDMS (α_a-process). Above 155 K, the dielectric strength $\Delta\epsilon$ of this process exhibits a stronger decrease by raising up the temperature while an additional relaxation process (α_{ac}-process) progressively grows up at lower frequencies. At 165 K, the α_a-process has completely disappeared, and only the α_{ac}-process remains. This additional peak is considerably broader than the α_a-process, and its dielectric strength is comparatively much weaker. It is well established[28−30] that the α_{ac}-process is induced by the PDMS cold crystallization: indeed, because of the formation of PDMS crystallites, a fraction of the chain segments within the amorphous parts are constrained and exhibit a different mobility than in the purely

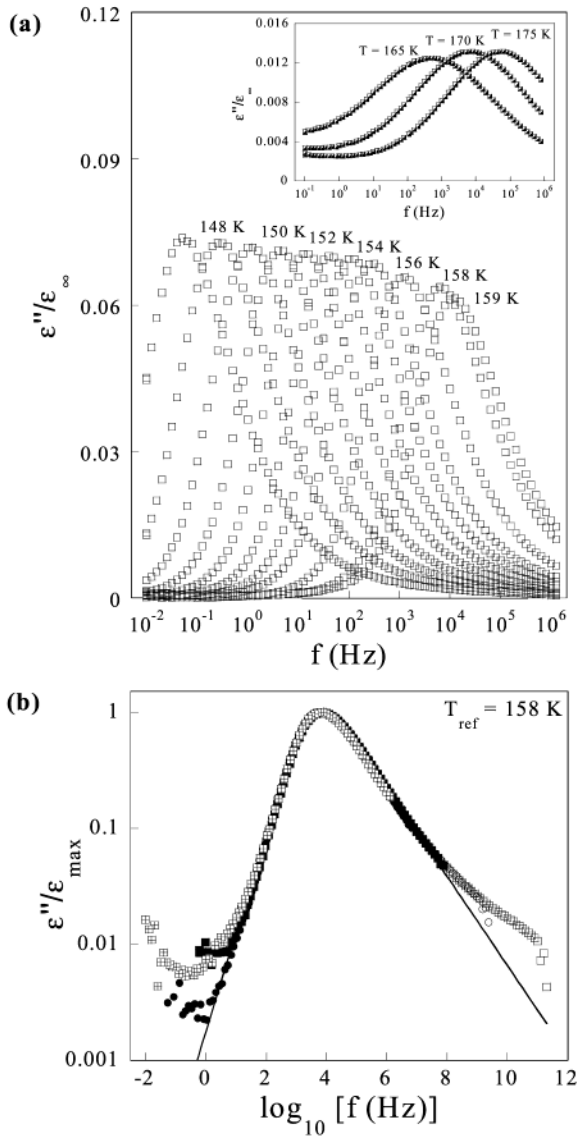

Figure 1. (a) Dielectric loss ϵ'' vs frequency for the amorphous PDMS homopolymer at selected temperatures between 147 and 159 K. Inset: dielectric loss ϵ'' vs frequency at 165, 170, and 175 K, corresponding to PDMS segments in the "rigid amorphous phase" resulting from cold crystallization during the heating run. The ϵ'' values were normalized according to the high-frequency permittivity ϵ_∞. (b) Master curve of ϵ'' for pure PDMS in the amorphous state, referenced to $T_{ref} = 158$ K, using data recorded at 147 (□), 150 (○), 153 (■), 156 (●) and 158 K (⊞). The solid line corresponds to the fit of the master curve by the Havriliak−Negami equation.

amorphous PDMS. The segmental motions within this so-called "rigid amorphous phase" (denoted as RAP) give rise to the α_{ac}-process. Thus, to characterize properly the dielectric response of pure amorphous PDMS above 155 K, $\epsilon^*(\omega)$ was measured at the desired temperature, immediately just after the quench of the sample in liquid nitrogen: by this way, measurements of $\epsilon^*(\omega)$ on the pure amorphous PDMS in the range $10^{-2}-10^7$ Hz were possible up to 159 K (see Figure 1a). For higher temperatures, cold crystallization occurs during the acquisition time so that in the following we limit our analysis of the dynamics in the amorphous PDMS to temperatures lower than 159 K.

The characteristic relaxation time τ for both α_a- and α_{ac}-processes is derived from the frequency f_{max} at the peak maximum ($\tau = 1/(2\pi f_{max})$). The temperature dependence of τ for both processes is reported in Figure 2. In both cases the evolution of τ with T is well described by the Vogel−Fulcher−Tamman (VFT) equation:

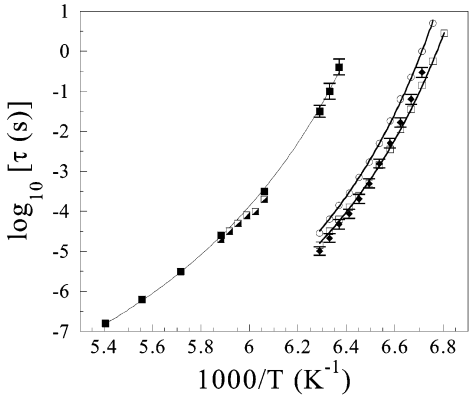

Figure 2. Arrhenius plot of the characteristic relaxation time τ, deduced from the frequency f_{max} of the dielectric loss maximum, for the PDMS homopolymer (□) and the PS−PDMS diblock (○) in the amorphous state. The temperature dependence of τ for PDMS in the "rigid amorphous phase", obtained after isothermal cold crystallization (■) and obtained during the progressive heating run (◪), is also included. The solid lines correspond to the fit of the experimental data using a VFT equation. The $\tau_{min}(T)$ variation (◆) is also reported for comparison (see text for details). Error bars smaller or comparable to the data point symbols are not represented.

Table 2. VFT Fit Parameters Obtained on the PDMS Homopolymer and on the PS−PDMS Diblock[a]

sample	relaxation process	D	T_0 (K)
PDMS	α_a	3.84 ± 0.03	130.0 ± 0.2
PDMS	α_{ac}	4.92 ± 0.08	132.8 ± 0.4
PS−PDMS	α_a	3.70 ± 0.03	131.7 ± 0.2

[a] The τ_∞ value was fixed to the one obtained on pure amorphous PDMS (i.e., log [τ_∞ (s)] ≈ −12.25).

$$\tau(T) = \tau_\infty \exp\left(\frac{DT_0}{T - T_0}\right) \quad (1)$$

where the prefactor τ_∞, the fragility parameter D, and the Vogel temperature T_0 are temperature-independent parameters. The values of τ_∞, D, and T_0 deduced from the fit of eq 1 to the experimental data are reported in Table 2. The VFT parameters for the α_a-process enable to estimate the so-called dielectric glass transition temperature, $T_{g,diel}$, of amorphous PDMS as defined by the condition $\tau(T_{g,diel}) \approx 100$ s: $T_{g,diel} \approx 145.2$ K ± 0.4 K, which is close to the calorimetric T_g value.

The dielectric loss $\epsilon''(\omega)$ recorded on pure amorphous PDMS was fitted according to the empirical Havriliak−Negami relaxation function[13,31]

$$\epsilon''(\omega) = -\Delta\epsilon \, \mathrm{Im}\left[\frac{1}{[1 + (i\omega/\omega_c)^\alpha]^\gamma}\right] \quad (2)$$

In this equation, α (γ) denotes the symmetric (asymmetric) broadening of the relaxation peak ($0 < \alpha, \gamma < 1$); $\Delta\epsilon$ is its dielectric strength, and ω_c is a characteristic frequency related to τ by following the equation[32]

$$\omega_c\left[\sin\left(\frac{\alpha\pi}{2(\gamma+1)}\right)\right]^{1/\alpha} = \tau^{-1}\left[\sin\left(\frac{\gamma\alpha\pi}{2(\gamma+1)}\right)\right]^{1/\alpha} \quad (3)$$

The shape parameters α and γ are found to be es-

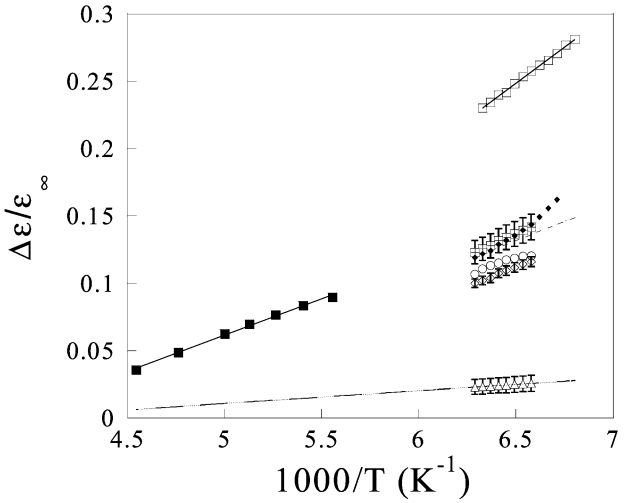

Figure 3. Reduced dielectric strength ($\Delta\epsilon/\epsilon_\infty$) vs inverse temperature for the α-process measured on a PDMS homopolymer in the amorphous state (□) and in the "rigid amorphous phase" induced by isothermal cold crystallization (■). The solid lines represent the linear fits of both sets of data. The dashed line corresponds to the fit of the data obtained on pure amorphous PDMS, rescaled according to the PDMS volume fraction in the PS−PDMS diblock ($\phi_{PDMS} = 0.53$). The dash−dotted line is the fit of the data obtained on the PDMS "rigid amorphous phase", rescaled according to the contribution of "rigid" PDMS segments in the diblock ($f = 0.18$). Reduced dielectric strength of the α-process of amorphous PDMS in the diblock: determined as $[\epsilon'(10^{-2}\ \text{Hz}) - \epsilon_\infty]/\epsilon_\infty$ (○) and determined as the sum (⊞) of a contribution from PDMS segments close to the interfaces with PS blocks (△) and a contribution from the segments in the inner lamellae (◇). The variation of $\Delta\epsilon_{dib}(T)$ (◆), deduced from the final fitting procedure (see eq 7), is also reported for comparison. See text for details. The error bars are smaller than or comparable to the size of the symbols, if not indicated otherwise.

sentially temperature independent in the measured range $\alpha \approx 0.84 \pm 0.02$ and $\gamma \approx 0.46 \pm 0.03$. As a result, the time−temperature superposition was successfully applied to the $\epsilon''(\omega)$ loss curves of amorphous PDMS as is shown in Figure 1b: the reported master curve was obtained from the superposition of data in temperature increments of 2−3 K between 148 and 158 K.

The temperature evolution of $\Delta\epsilon/\epsilon_\infty$ is displayed in Figure 3, where the $\Delta\epsilon$ values were deduced from the fitting procedure while ϵ_∞ was taken as the component of $\epsilon'(\omega)$ at high frequency (1 MHz) and low temperature ($T = 147$ K). The accurate measurement of the $\Delta\epsilon$ values suffers from the incertitude on the determination of the geometric parameters (thickness and section) of the sample capacitor. However, as $\Delta\epsilon$ and ϵ_∞ should follow the same dependence on the sample dimensions, the systematic normalization of the $\epsilon''(\omega)$ data by ϵ_∞ enables to get a more precise comparison among the dielectric strength values of the samples studied. Thus, the unrelaxed permittivity ϵ_∞ should ideally be determined for each temperature investigated. However, because of the experimental limitation of the accessible frequency range, this measurement was not possible since for temperatures above 153 K, the $\epsilon'(\omega)$ curve has not achieved its plateau value at 1 MHz. Thus, we have assumed the temperature variation of ϵ_∞ to be negligible, and its value at 147 K was used for the normalization of $\Delta\epsilon$. As expected, $\Delta\epsilon/\epsilon_\infty$ decreases by raising the temperature, and in a first approach, the experimental behavior is well captured by means of a linear function of the reciprocal temperature. This monotonic variation, which is in agreement with the Onsager−Kirkwood−Fröhlich equation,[13] together with the temperature independence of the shape parameters, confirms that no cold crystallization occurs during the measurement time, particularly in the range 155−159 K.

Previous dielectric measurements on PDMS homopolymers have been performed, but most of them concern chains with rather low molecular weight.[28−30,33] In particular, the work of Kremer et al. has shown that for linear chains shape exponents are unaffected by the chain length N while the characteristic relaxation time and the dielectric strength tend to be constant for $N > 92$.[29] The values we have obtained for α, γ, τ, and $\Delta\epsilon$ on the PDMS homopolymer ($N = 218$) were compared to data in the molecular weight independent regime, and a good agreement was found.

3.2. PS−PDMS Diblock. The dielectric loss spectra $\epsilon''(\omega)$ obtained on the fully amorphous PS−PDMS diblock under isothermal conditions are plotted in Figure 4a for temperatures between 147 and 159 K. The characteristic relaxation time τ was obtained in the same way than for the homopolymer. Its temperature dependence is shown in Figure 2, and the VFT parameters are reported in Table 2. By comparison with the homopolymer, a shift of τ toward the higher relaxation times is clearly detected in the diblock. This shift is found to be of about 1 decade at $T = 148$ K, but it decreases when the temperature is raised. Accordingly, the dielectric glass transition temperature $T_{g,diel}$ is found to be higher in the diblock than in the homopolymer: $T_{g,diel} \approx 146.6 \pm 0.4$ K. It is worthy of remark that even though the experimental τ values can be also well described using a VFT fit with one of the parameters (τ_∞, for instance) fixed to the value obtained on the homopolymer, $T_{g,diel}$ was found to remain unchanged.

The α-relaxation of amorphous PDMS in the PS−PDMS diblock displays a significant broadening when the temperature is decreased. However, it has to be noted that the high-frequency slope of $\epsilon''(\omega)$ remains constant with temperature. For comparison, the dielectric loss curve $\epsilon''(\omega)$ obtained on the PDMS homopolymer in the amorphous state at $T = 158$ K is also reported in Figure 4c. The comparison shows that the high-frequency behavior observed in the diblock is the same than for the homopolymer: $\alpha\gamma \approx 0.39$. On the other hand, in contrast to the homopolymer case, the dielectric loss $\epsilon''(\omega)$ recorded on the diblock exhibits a wide extension toward the low frequencies, as can be seen in Figure 4. This extension is so large that even at $T = 159$ K it is not possible to capture the whole low-frequency side of the α-process. At this stage, it has to be emphasized that this low-frequency tail is an intrinsic part of the dielectric response of amorphous PDMS within the diblock: it does not originate from the contribution of a PDMS rigid amorphous phase, induced by cold crystallization, which would superimpose with the contribution of the remaining amorphous PDMS. Indeed, we have first checked that the low-frequency part of the $\epsilon''(\omega)$ curves, measured within the temperature range 147−159 K, was reproducible. Then, between 154 and 159 K, the isothermal $\epsilon''(\omega)$ measurement at a given temperature T was programmed at different times among successive isothermal acquisitions at other temperatures. The comparison of the different spectra obtained for this given temperature T via this procedure enables to detect when cold crystal-

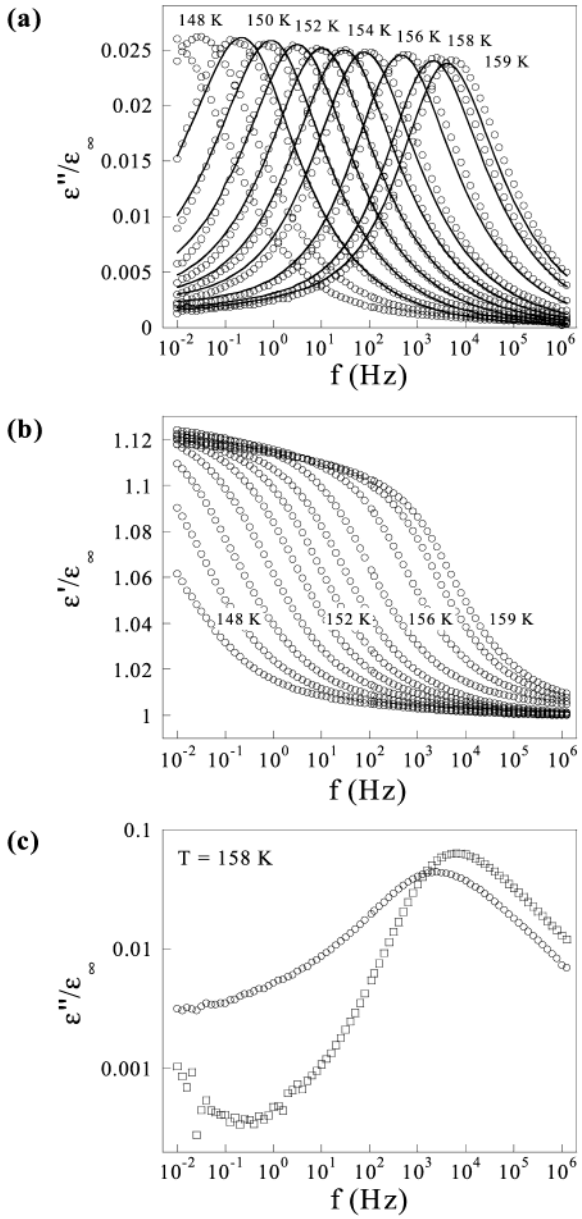

Figure 4. (a) Imaginary part ϵ'' and (b) real part ϵ' of the dielectric permittivity vs frequency for PDMS within the amorphous PS−PDMS diblock at various temperatures between 147 and 159 K. The ϵ'' and ϵ' values were normalized according to the high-frequency permittivity ϵ_∞. The solid lines hold for the description of the experimental data achieved according to the proposed model (see text for details). (c) Comparison of the normalized dielectric loss, $\epsilon''/\epsilon_\infty$, obtained at 158 K on the pure amorphous diblock (○) with that measured on the amorphous PDMS homopolymer (□) at the same temperature.

lization occurs and affects the $\epsilon''(\omega)$ curves. By this way, the dielectric data reported in Figure 4 can be surely attributed to the pure amorphous PDMS within the diblock.

Using the molecular characteristics of the diblock as determined by GPC (see Table 1) and assuming density values within the PDMS and PS sublayers to be close to the bulk values ($\rho_{PDMS(D)} \approx 1.053$ g cm^{-3}; $\rho_{PS} \approx 1.044$ g cm^{-3}),[34] the PDMS volume fraction ϕ_{PDMS} is estimated to be about 53%. Thus, the expected dielectric strength $\Delta\epsilon_{dib}$ in the diblock should be roughly equal to $0.53\Delta\epsilon$ (see the corresponding dashed line in Figure 3). However, experimentally, the dielectric strength $\Delta\epsilon_{dib}$ cannot be rigorously extracted from the dielectric curves reported in Figure 4a. Indeed, even for the highest temperature considered (159 K), the dielectric loss $\epsilon''(\omega)$ still displays nonzero components for frequencies close to 10^{-2} Hz. Correspondingly, after a strong increase when the frequency decreases down to f_{max}, the real part $\epsilon'(\omega)$ does not exhibit a plateau for lower frequencies: a weak, but continuous, increase is observed (see Figure 4b). Thus, we decided to estimate the fraction of dipoles relaxing within the probed spectral window (10^{-2}−10^7 Hz) by determining the quantity $[\epsilon'(10^{-2}\text{ Hz}) - \epsilon_\infty]/\epsilon_\infty$ (see open circles in Figure 3). The latter was evaluated at temperatures for which the strong increase in ϵ' close to f_{max} is well captured within 10^{-2}−10^7 Hz. The corresponding values are smaller than $0.53\Delta\epsilon/\epsilon_\infty$ (as expected according to the PDMS segment concentration in the sample), but the observed relative deviation, in the temperature range where the main part of the loss peak is within the experimental window, is of about 10% only: therefore, most of the dipoles within the PDMS sublayers relax within the experimental spectral window in the temperature range considered. This is supported by the similar temperature dependence of $[\epsilon'(10^{-2}\text{ Hz}) - \epsilon_\infty]/\epsilon_\infty$ at high temperatures as compared with $0.53\Delta\epsilon/\epsilon_\infty$. Thus, the differences between $[\epsilon'(10^{-2}\text{ Hz}) - \epsilon_\infty]/\epsilon_\infty$ and $0.53\Delta\epsilon/\epsilon_\infty$ can be attributed to the fact that even for the highest temperatures investigated, the PDMS relaxation in the diblock contributes to frequencies lower than 10^{-2} Hz (see Figure 4).

4. Data Analysis

A major difference between the relaxation behavior of the PDMS homopolymer and PDMS in the diblock is the low-frequency contribution observed in the latter. A possible way to interpret such differences is to consider that, in the PDMS layers of the PS−PDMS diblock, the chain segments located close to the interfaces with the PS rigid blocks display a different dynamical behavior with respect to the segments located in the inner of the lamellae. In particular, their reorientational motions would be comparatively slower[26] due to the effect of the anchorage to the PS solid walls. In that context, it appears physically reasonable to attribute the very low-frequency components of the $\epsilon''(\omega)$ curves recorded on the diblock to PDMS chain segments close to PS blocks. On the contrary, in the middle of the lamellae, the PDMS monomer units are surrounded by other PDMS chain segments and thus should experience a friction coefficient similar to that in the PDMS homopolymer. Thus, these monomer units should display a dielectric behavior similar to that of the homopolymer. In particular, no contribution from faster relaxation processes is expected within the PDMS layers: this feature may rationalize the fact that the high-frequency side of the α-peak in the diblock is quite similar to the one observed on the homopolymer.

In the following, we develop a simplified approach to analyze our dielectric data to get a deeper understanding of the segmental dynamics within the PDMS layers. For this purpose, let us consider first the case of the rigid amorphous phase (RAP) within a semicrystalline PDMS homopolymer. Above the calorimetric glass transition T_g, this phase consists of disordered PDMS chain portions anchored to "rigid" crystallites wherein other parts of the chain are immobilized.[35] Because of this anchorage, the chain segment reorientational motions in the RAP are restricted, resulting in changes in their

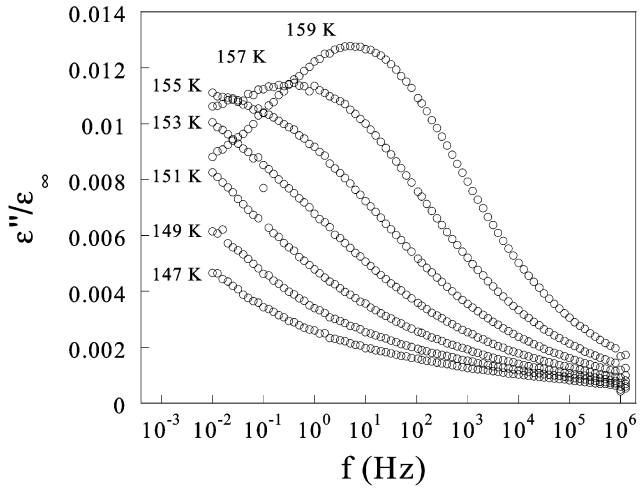

Figure 5. Frequency dependence of the dielectric loss ϵ'' recorded on the "rigid amorphous phase" (RAP) of the PDMS homopolymer at various temperatures in the range 147−159 K. The considered RAP was obtained after a cold crystallization of PDMS, initially in the amorphous state, at $T = 160$ K for 7 h.

local dynamics as compared with those in amorphous PDMS. In a similar way, the anchorage of the PDMS chains to the glassy PS layers in the PS−PDMS diblock should induce (above the calorimetric glass transition of the PDMS blocks) segmental motions of the PDMS monomer units close to the PS solid walls different from those in the inner lamellae. At this stage, it is worth remarking that the segmental dynamics involves a typical length scale of the order of a few nanometers and should not be greatly influenced by the chain segments located at greater distances. At the scale of a few nanometers, PDMS segments close to glassy PS blocks and PDMS segments close to PDMS crystallites should not display great differences in their dynamics. If the most relevant feature governing the PDMS segmental dynamics is the presence of anchoring junctions to "rigid" components, it is physically reasonable to describe the dynamical behavior of the PDMS monomer units close to the PS solid blocks by assuming that the corresponding dielectric response is similar to that of the RAP within the semicrystalline PDMS homopolymer.

Additionally, we have also performed a detailed study of the crystallization properties within the PDMS sublayers of PS−PDMS diblocks by comparison with PDMS homopolymers.[36] According to these data concerning the crystallization kinetics, the isothermal cold crystallization of the PDMS homopolymer was carried out at 160 K for 7 h, and then the dielectric loss $\epsilon''(\omega)$ was monitored. The results obtained between 147 and 159 K are shown in Figure 5. It appears that for the so cold-crystallized sample no contribution from amorphous PDMS can be detected (compare Figure 1a and Figure 5).

When the low-frequency part of the dielectric losses in the diblock at high temperatures is compared with that obtained in the cold-crystallized PDMS, it is found that they display a remarkable similarity. This is illustrated in Figure 6a, wherein a good matching of the low-frequency components of the $\epsilon''(\omega)$ spectra recorded at 159 K on both the rigid amorphous phase of the homopolymer (denoted as $[\epsilon''(\omega)]_{RAP}$) and the diblock (denoted as $[\epsilon''(\omega)]_{dib}$) was obtained. The rescaling factor f applied to the $[\epsilon''(\omega)]_{RAP}$ data to achieve this matching

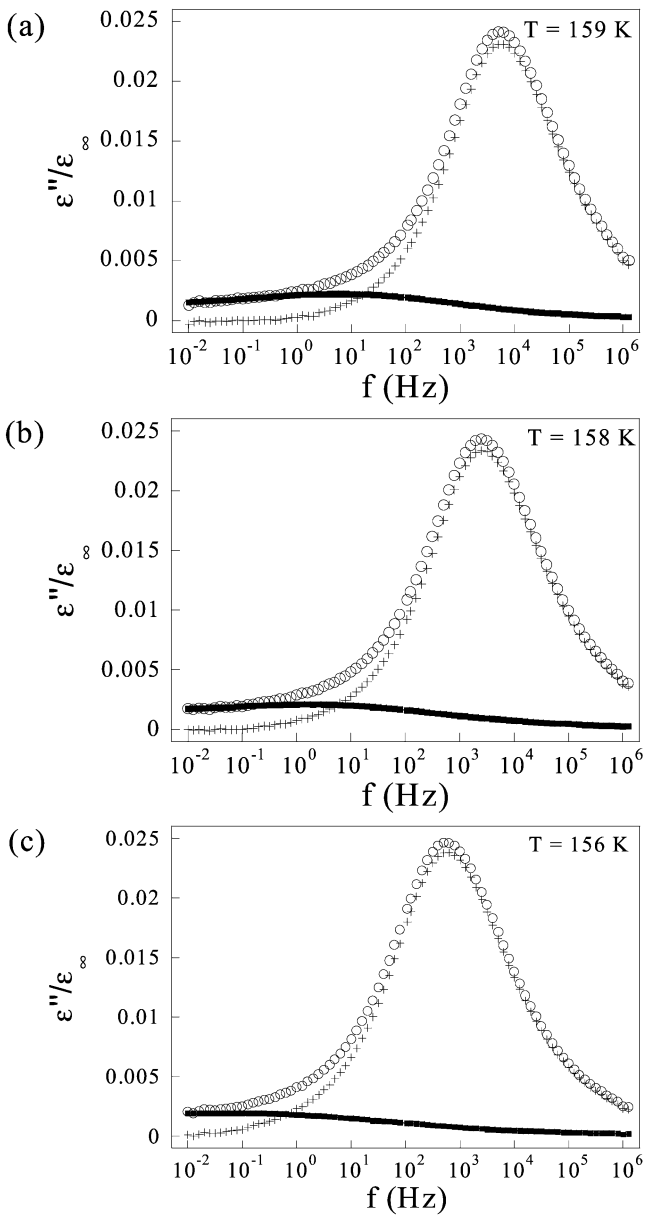

Figure 6. Decomposition of the dielectric loss $[\epsilon''(\omega)]_{dib}$ (○) obtained on the amorphous PS−PDMS diblock in two components: (1) the $[\epsilon''(\omega)]_{RAP}$ spectrum recorded at the same temperature on the "rigid amorphous phase" resulting from cold crystallization of pure PDMS, multiplied by a factor f (■); (2) the remaining dielectric signal $[\epsilon''(\omega)]_{inner} = [\epsilon''(\omega)]_{dib} - f[\epsilon''(\omega)]_{RAP}$ (+). The fraction f, determined at $T = 159$ K to match the low-frequency side of $f[\epsilon''(\omega)]_{RAP}$ with that of $[\epsilon''(\omega)]_{dib}$, is maintained constant at lower temperatures.

was of about 0.18. In our view, this factor f would be related to the fraction of segments, likely attached to the PS walls, displaying a segmental dynamics qualitatively different from that one of the chain segments in the inner lamellae. In this framework, the factor f is expected to be nearly unaffected by varying the temperature from 147 to 159 K. Thus, imposing f to the value obtained at 159 K, a comparison of $[\epsilon''(\omega)]_{dib}$ with $f[\epsilon''(\omega)]_{RAP}$ was performed at lower temperatures: between 154 and 158 K, the $f[\epsilon''(\omega)]_{RAP}$ spectra enable to describe satisfactorily the low-frequency part of the dielectric loss $[\epsilon''(\omega)]_{dib}$, as shown in Figures 6b,c. Note that below 154 K the contribution of the chain segments in the inner lamellae to the α_a-process shifts toward low frequency and superimposes with the dielectric signal

expected from the monomers close to the PS blocks, making the low-frequency values of $[\epsilon''(\omega)]_{dib}$ higher than those of $f\,[\epsilon''(\omega)]_{RAP}$.

The similarities of the low-frequency part between $[\epsilon''(\omega)]_{dib}$ and $f\,[\epsilon''(\omega)]_{RAP}$, first at 159 K and then at lower temperatures using a fixed f value, are consistent with the proposed approach for the data analysis quoted above. A more critical test concerns the dielectric strength of the α_a-process. As already mentioned in section 3.2, the dielectric strength $\Delta\epsilon_{dib}$ related to the PDMS α_a-process in the diblock cannot be exactly determined experimentally in the probed frequency range $10^{-2}-10^{7}$ Hz. The expected values, however, are given by $0.53\Delta\epsilon$, $\Delta\epsilon$ being the dielectric strength measured on the homopolymer. Thus, if our approach is correct, the sum of the dielectric strength related to the $f\,[\epsilon''(\omega)]_{RAP}$ spectrum and the one related to the rest ($[\epsilon''(\omega)]_{dib} - f\,[\epsilon''(\omega)]_{RAP}$) should be close to $0.53\Delta\epsilon$.

The dielectric strength related to the PDMS segments close to the PS walls is equal to $f\,\Delta\epsilon_{RAP}$. Of course, in the temperature range of interest (147−159 K), the α_{ac}-process occurs out of our spectral window (peak maximum below 10^{-2} Hz, see Figure 5), and thus, the $\Delta\epsilon_{RAP}$ values between 147 and 159 K were obtained by extrapolating the $\Delta\epsilon_{RAP}$ values measured between 180 and 220 K, assuming a linear dependence with respect to $1/T$. These extrapolated values are reported in Figure 3 in the range 147−159 K (up triangles). On the other hand, the dielectric response of the chain segments within the inner lamellae, denoted as $[\epsilon''(\omega)]_{inner} = [\epsilon''(\omega)]_{dib} - f\,[\epsilon''(\omega)]_{RAP}$, is fully captured within the spectral window $10^{-2}-10^{7}$ Hz, for temperatures between 152 and 159 K (see Figure 6 for some temperatures). The $[\epsilon''(\omega)]_{inner}$ curves can be satisfactorily fitted by means of the empirical Havriliak−Negami function, and the corresponding dielectric strength, obtained for these temperatures, is reported in Figure 3 as diamonds. Clearly, it can be observed that the sum (crossed squares) of $f\,\Delta\epsilon_{RAP}$ (up triangles) with $\Delta\epsilon_{inner}$ (diamonds) is very close to the expected $0.53\Delta\epsilon$ values (dashed line). This finding indicates that describing the dynamics of the PDMS monomers close to the PS blocks using the dielectric response of the RAP within a semicrystalline PDMS is well-consistent with the amount of dipoles relaxing at frequencies below 10^{-2} Hz in the PDMS layers of the diblock.

The temperature evolution of the $[\epsilon''(\omega)]_{inner}$ curves is reported in Figure 7a, while in Figure 7b, the loss curve $[\epsilon''(\omega)]_{inner}$ at 158 K is compared with the dielectric loss measured at the same temperature on the amorphous PDMS homopolymer. The amplitude of this latter was multiplied by a scaling factor to compare the high-frequency behavior of both peaks. As can be seen in Figure 7b, a good matching can be obtained, indicating that the high-frequency side of the dielectric loss $[\epsilon''(\omega)]_{inner}$ displays a similar frequency dependence than the one of the α_a-peak in the amorphous homopolymer. However, the comparison with the loss curve of the PDMS homopolymer also shows that the segmental dynamics within the inner lamellae still differs from the one occurring in the "bulk" state. Indeed, a significant and temperature-dependent extension of the peak toward the low frequencies remains for the inner lamellae of the diblock.

Finally, our dielectric approach enables to estimate the contribution of the segments involved in the "RAP-like" regions. At $T = 158$ K, the ratio $f\,\Delta\epsilon_{RAP}/\Delta\epsilon_{dib}$ suggests that about 18% of the PDMS monomers within the layer exhibit a dynamical behavior similar to the RAP phase of a semicrystalline PDMS. Moreover, the ratio of the dielectric strength of the rescaled PDMS α_a-peak at 158 K to the dielectric strength related to $[\epsilon''(\omega)]_{inner}$ at the same temperature (see Figure 7b) is an approximate way to estimate the amount of PDMS segments that would give a dielectric contribution similar to that recorded on the pure amorphous PDMS: about 59% in the present case. The remaining 23% segments, within the inner lamella, would contribute with intermediate time scales. All this shows that in the PS−PDMS diblock a significant gradient of mobility occurs.

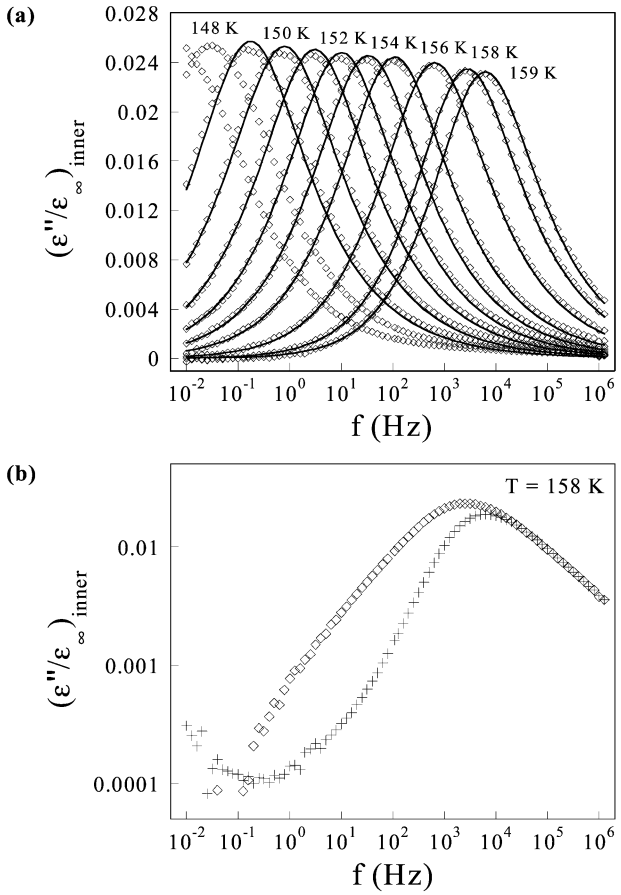

Figure 7. (a) Dielectric loss $[\epsilon''(\omega)]_{inner}$, normalized according to the high-frequency permittivity ϵ_∞, attributed to the "inner" lamellae of the PDMS layers, in the amorphous state, within the PS−PDMS diblock for temperatures between 147 and 159 K. (b) Comparison of the normalized dielectric loss $[\epsilon''(\omega)]_{inner}/\epsilon_\infty$ obtained at 158 K (◇) with that of the amorphous PDMS homopolymer at the same temperature (+). The amplitude of the latter has been rescaled to match the high-frequency side of the $[\epsilon''(\omega)]_{inner}$ peak.

5. Discussion

We have shown above that in the PS−PDMS diblock the $\epsilon''(\omega)$ curves could be well described assuming two types of PDMS segments depicting qualitatively distinct segmental dynamics. For the first type, the dielectric response can be represented by assuming the same shape and time scale as the segments in the amorphous constrained phase of a cold-crystallized PDMS homopolymer. This contribution to the dielectric response would likely originate from PDMS segments attached to the PS walls. The other type of PDMS segments

seems to display a dielectric response qualitatively similar to that observed in the pure amorphous PDMS homopolymer. According to our analysis, the quantitative differences that remain between the segmental dynamics of this second type of PDMS segments and the one in the amorphous homopolymer should be attributed to a gradient of mobility occurring inside the lamellae. Indeed, the chain segments located in the inner lamellae, in the direct vicinity of the PDMS "RAP-like" population, should be comparatively more mobile, but their reorientational motions are however restricted by the neighboring "RAP-like" segments. Thus, as the distance between the considered monomer units and the PS/PDMS interface increases, the influence of the anchorage to the PS solid walls on the PDMS segmental motions should decrease and the characteristic relaxation time is expected to approach progressively the bulklike value. Under these conditions, if the lamellar thickness is high enough, the segmental dynamics in the center of the lamellae should be similar to that one observed in the "bulk" PDMS. This interpretation is consistent with the low-frequency extension exhibited by the $[\epsilon''(\omega)]_{inner}$ curves—by comparison with the homopolymer—and consistent with the observed similarity in the high-frequency slope between diblock and pure PDMS.

A way to model such a situation could be derived from the procedure used to account for the dynamical heterogeneity of each component in miscible polymer blends.[37] Thus, we may consider that the PDMS inner lamella is divided in various fictive regions and assume that the PDMS segments within each of these regions display a dielectric behavior similar to that one in pure amorphous PDMS, but with a characteristic relaxation time depending on the region considered. According to section 3.1, the dielectric response in each region can be modeled by a Havriliak−Negami function (see eq 2), the parameters α and γ being fixed to 0.84 and 0.46, respectively. In that framework, the $[\epsilon''(\omega)]_{inner}$ curves can be expressed as

$$[\epsilon''(\omega)]_{inner} = \Delta\epsilon_{inner}\int_{\tau_{min}}^{+\infty} \mathrm{Im}\left[\frac{-1}{[1+(i\omega/\omega_c)^{\alpha}]^{\gamma}}\right] g(\log\tau)\, d(\log\tau) \quad (4)$$

the relaxation time distribution $g(\log\tau)$ being normalized. Here, following our physical description, the limit time τ_{min} should correspond to the relaxation time of the segmental dynamics in bulk PDMS. In a first approach, we propose a simple form for $g(\log\tau)$

$$g(\log\tau) \propto \exp\left[-b\,\log\left(\frac{\tau}{\tau_{min}}\right)\right] \quad (5)$$

b being a shape parameter. The fitting of the $[\epsilon''(\omega)]_{inner}$ curves according to eqs 4 and 5 was performed between 149 and 159 K, as shown in Figure 7a. In the fitting procedure used, the dielectric strength $\Delta\epsilon_{inner}$, for each temperature, was set equal to the value deduced from the fit of the $[\epsilon''(\omega)]_{inner}$ spectrum by a Havriliak−Negami function. A rather good agreement was found between the experimental and the fitting curves, thus validating the proposed form as a good approximate of the distribution $g(\log\tau)$. The obtained distributions are shown in Figure 8. The temperature dependence of τ_{min} (one of the two fitting parameters) is reported in Figure 2: the $\tau_{min}(T)$ variation is found to display a rather good

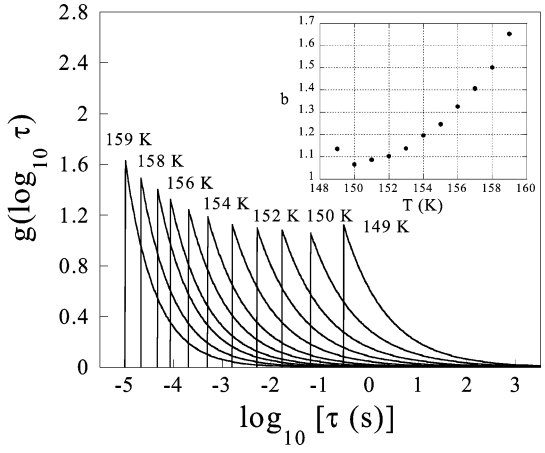

Figure 8. Distributions of relaxation times, $g(\log\tau)$, describing the dynamics of the PDMS segments within the "inner" lamellae of the PS−PDMS diblock (amorphous state) for various temperatures between 149 and 159 K. The temperature variation of the parameter accounting for the distribution broadening is depicted in the inset.

matching with the $\tau(T)$ evolution measured on the pure amorphous PDMS homopolymer, which is consistent with the physical picture developed above. The other free parameter, b, is found to decrease with temperature (see inset in Figure 8), which is consistent with the narrowing of the $[\epsilon''(\omega)]_{inner}$ curves observed in Figure 7a, when the temperature is raised. It is worthy to note that the expression for $g(\log\tau)$ proposed above (see eq 5) is not the only one possible. However, in our first approach to capture the main features of the segmental dynamics within the amorphous PS−PDMS diblock, this simple form, in qualitative agreement with the experimental findings, was retained in order to limit the number of free parameters involved in the fitting procedure. For the same reason, we have assumed the variations of the shape parameters α and γ to be negligible within the inner lamella. Of course, such α- and γ-variations could also contribute to the extension of the $[\epsilon''(\omega)]_{inner}$ curves toward low frequencies.

At this stage of the discussion, it would be of interest to explain the occurrence of the detected relaxation time distributions. The mobility gradients of the PDMS segments belonging to the different regions in the inner lamella could be related with the different molecular packings, the differences being induced by the chain constraints. The fact that the minimum time of the distribution corresponds approximately to the relaxation time in pure PDMS suggests that, likely in regions located in the center of the lamellae, the packing of the PDMS segments is similar to that in the pure PDMS homopolymer, the packing density increasing in the other regions due to the anchorage of the PDMS chains to the PS blocks. Recent dielectric studies of relaxation dynamics in glass-forming systems (including polymers) have evidenced that in most cases the pressure dependence of the relaxation time τ can be described by considering the Vogel temperature T_0 to be the single pressure-dependent parameter of the VFT equation (see eq 1).[38] In that context, the relationship between pressure and molecular packing may suggest to interpret the relaxation time distribution $g(\log\tau)$ within the PDMS inner lamellae as originating from differences in molecular packing and consequently from a distribution of the parameter T_0.

Thus, we have obtained the corresponding distribution of T_0 from the distribution $g(\log\tau)$ previously

deduced at a particular temperature ($T = 152$ K) using the VFT equation (see eq 1), both parameters τ_∞ and D being fixed to the values determined on pure PDMS in the supercooled melt state (see Table 2). A convenient analytical description for this T_0 distribution is

$$h(T_0) \propto \exp(-0.6074(T_0 - 128.53)) \qquad (6)$$

This T_0 distribution would characterize, at least approximately, the gradients of molecular packing in the inner lamellae. Again, other forms of $h(T_0)$ could be used to give account to our experimental data, and the expression quoted above (see eq 6) has been retained for the sake of simplicity.

All the previous arguments lead us to propose the following simple picture for the segmental dynamics within the PDMS layers. The anchorage of the PDMS chains to the PS glassy blocks imposes, for some of the segments, a dynamical behavior similar to that one observed in the amorphous constrained phase of a semicrystalline PDMS homopolymer (characterized by the dielectric response $[\epsilon''(\omega)]_{RAP}$). The contribution of such PDMS segments to the dielectric relaxation has been estimated to be about $\lambda = 18\%$. However, it is difficult to estimate the corresponding amount of monomeric units because of the possible effect of the anchorage which limits the dipole reorientations. Thus, a reasonable value for the fraction of PDMS units in such a situation could be in the range 15%−25%. The segmental dynamics of the other PDMS segments in the lamellae (about 75%−85%) suggests pronounced gradients of molecular packing, which we have characterized by a T_0 distribution, $h(T_0)$. Except this difference in the T_0 parameter, the dielectric behavior of these segments can be considered to be similar to that in the supercooled melt. Using all these features, it is possible to build up the dielectric loss curves that should be obtained in this framework and compare them to the experimental measurements. Indeed, the $\epsilon''(\omega)$ curves within this simple picture can be calculated through the equation

$$\epsilon''(\omega) = \Delta\epsilon_{dib}\left\{\lambda \frac{1}{\Delta\epsilon_{RAP}}[\epsilon''(\omega)]_{RAP} + (1-\lambda)\int_{128.53\ K}^{+\infty} \mathrm{Im}\left[\frac{-1}{[1 + (i\omega/\omega_c(T_0))^{\alpha}]^{\gamma}}\right] h(T_0)\, dT_0\right\} \qquad (7)$$

Here, $\Delta\epsilon_{dib}$ is a free parameter. The comparison between calculated and experimental dielectric losses obtained in the diblock is illustrated in Figure 4a. The temperature dependence of the corresponding $\Delta\epsilon_{dib}$ values, reported in Figure 3 (filled diamonds), shows a rather good matching with the expected $\Delta\epsilon_{dib}$ values ($0.53\Delta\epsilon$). As can be seen in Figure 4a, a satisfactory agreement is found, suggesting that our model, even simplistic, captures the main effects of the diblock structure on the PDMS segmental dynamics.

The good agreement between the calculated curves and the experimental data suggests that considering the dynamics of the PDMS segments inside each regions to be similar to that one in pure PDMS is a rather good approximation. Taking into account the thickness of the lamellae (about 10 nm), the typical size of these regions would be of the order of or less than 1 nm. This would suggest that the relevant length scale for the PDMS segmental dynamics should be shorter than 1 nm over the whole temperature range probed, including the glass transition one.

Last, it is of interest to compare our results with those previously obtained on other systems of confined PDMS chains. Schönhals et al. have recently combined dielectric spectroscopy, temperature-modulated DSC, and neutron scattering experiments to probe the segmental dynamics of PDMS oligomers within uncoated silica-based nanoporous glasses.[23] A significant speeding up of the segmental dynamics was observed when the pore size was lowered below 25 nm. However, in these systems, the PDMS chains can diffuse freely within the pores, by contrast with the PDMS chains of the diblock studied herein. In addition, the difference of chain length (oligomers in the work by Schönhals et al. vs chains in the regime for which the dielectric α_a-peak is independent of molecular weight in the diblock) as well as the difference of confinement dimensionality (3D for nanopores vs 1D in the diblock) makes also the comparison with our data rather complex. A closer situation is encountered in PDMS grafted films. In particular, Kremer et al. have performed dielectric measurements on PDMS brushes having a thickness higher than the unperturbed radius of gyration $R_{g,0}$ of the considered chains.[24] This situation is similar in the PS−PDMS diblock: the PDMS chains are anchored to the PS glassy blocks, and the thickness of the PDMS layers is also slightly higher than $R_{g,0}$. In both cases, a comparable shift of the α_a-relaxation toward low frequencies, by comparison with the "bulk" state, is observed. It is probable that, for PDMS chains within grafted films of sufficiently high thickness as for PDMS chains within the diblock, the segmental dynamics is mainly governed by the chain anchorage: confinement effects would not occur or would be too weak to affect significantly the segmental motions.

6. Conclusions

The segmental dynamics of amorphous PDMS in a PS−PDMS lamellar diblock was investigated by means of broadband dielectric spectroscopy. Our results show that the main relevant features governing the PDMS segmental motions within the layers originate from the chain anchorage to the glassy PS blocks. This constraint imposes a specific dynamical behavior for the segments close to the interface as well as a gradient of mobility for the other segments. By contrast, confinement effects, imposed by the geometric space restriction of the PDMS chains, do not seem to play a significant role at the length scale probed by the α-relaxation process.

The proposed picture should be applied and compared with experimental data obtained on other lamellar structures: PS−PDMS diblocks with various PDMS chain lengths and/or a PS−PDMS−PS triblock consisting of two chains of the diblock presently studied, linked by their PDMS extremities. Such investigations are currently in progress.

Acknowledgment. The authors thank the University of the Basque Country (Project No. 9/UPV00206.215-13568/2001) and the Spanish Ministry of Science and Technology (Project No. MAT 2001/0070) for their support. The support from "Donostia International Physics Center" is also acknowledged. The authors are also grateful to Dr. Philippe Auroy (Institut Curie, Paris) for synthesizing and characterizing the samples.

References and Notes

(1) Hamersky, M. W.; Tirrell, M.; Lodge, T. P. *Langmuir* **1998**, *14*, 6974.

(2) Lodge, T. P.; Dalvi, M. C. *Phys. Rev. Lett.* **1995**, *75*, 657.
(3) Rittig, F.; Fleischer, G.; Kärger, J.; Papadakis, C. M.; Almdal, K.; Stepanek, P. *Macromolecules* **1999**, *32*, 5872.
(4) Yokoyama, H.; Kramer, E. J. *Macromolecules* **1998**, *31*, 7871.
(5) Stühn, B.; Stickel, F. *Macromolecules* **1992**, *25*, 5306.
(6) Alig, I.; Floudas, G.; Avgeropoulos, A.; Hadjichristidis, N. *Macromolecules* **1997**, *30*, 5004.
(7) Floudas, G.; Paraskeva, S.; Hadjichristidis, N.; Fytas, G.; Chu, B.; Semenov, A. N. *J. Chem. Phys.* **1997**, *107*, 5502.
(8) Kyritsis, A.; Pissis, P.; Mai, S.-M.; Booth, C. *Macromolecules* **2000**, *33*, 4581.
(9) Dollase, T.; Graf, R.; Heuer, A.; Spiess, H. W. *Macromolecules* **2001**, *34*, 298.
(10) Valic, S.; Deloche, B.; Gallot, Y.; Skoulios, A. *Polymer* **1995**, *36*, 3041.
(11) Vogt, S.; Gerharz, B.; Fischer, E. W.; Fytas, G. *Macromolecules* **1992**, *25*, 5986.
(12) Hoffmann, A.; Koch, T.; Stühn, B. *Macromolecules* **1993**, *26*, 7288.
(13) Kremer, F.; Schönhals, A. *Broadband Dielectric Spectroscopy*; Springer-Verlag: Berlin, Germany, 2003.
(14) Hadjichristidis, N.; Pispas, S.; Floudas, G. *Block Copolymers: Synthetic Strategies, Physical Properties, and Applications*; Wiley-Interscience: Hoboken, NJ, 2003; Chapter 20.
(15) Karatasos, K.; Anastasiadis, S. H.; Floudas, G.; Fytas, G.; Pispas, S.; Hadjichristidis, N.; Pakula, T. *Macromolecules* **1996**, *29*, 1326.
(16) Watanabe, H. *Macromolecules* **1995**, *28*, 5006.
(17) Karatasos, K.; Anastasiadis, S. H.; Pakula, T.; Watanabe, H. *Macromolecules* **2000**, *33*, 523.
(18) Watanabe, H. *Prog. Polym. Sci.* **1999**, *24*, 1253.
(19) Yao, M. L.; Watanabe, H.; Adachi, K.; Kotaka, T. *Macromolecules* **1991**, *24*, 2955.
(20) Floudas, G.; Paraskeva, S.; Hadjichristidis, N.; Fytas, G.; Chu, B.; Semenov, A. N. *J. Chem. Phys.* **1997**, *107*, 5502.
(21) Floudas, G.; Meramveliotaki, K.; Hadjichristidis, N. *Macromolecules* **1999**, *32*, 7496.
(22) Zhukov, S.; Geppert, S.; Stühn, B.; Staneva, R.; Ivanova, R.; Gronski, W. *Macromolecules* **2002**, *35*, 8521.
(23) Schönhals, A.; Goering, H.; Schick, C.; Frick, B.; Zorn, R. *Eur. Phys. J. E* **2003**, *12*, 173.
(24) Kremer, F.; Hartmann, L.; Serghei, A.; Pouret, P.; Léger, L. *Eur. Phys. J. E* **2003**, *12*, 139. Hartmann, L.; Kremer, F.; Pouret, P.; Léger, L. *J. Chem. Phys.* **2003**, *118*, 6052.
(25) Zhukov, S.; Geppert, S.; Stühn, B.; Staneva, R.; Gronski, W. *Macromolecules* **2003**, *36*, 6166.
(26) Lorthioir, C.; Auroy, P.; Deloche, B.; Gallot, Y. *Eur. Phys. J. E* **2002**, *7*, 261.
(27) Rosati, D.; Perrin, M.; Navard, P.; Harabagiu, V.; Pinteala, M.; Simionescu, B. C. *Macromolecules* **1998**, *31*, 4301.
(28) Adachi, H.; Adachi, K.; Ishida, Y.; Kotaka, T. *J. Polym. Sci., Part B: Polym. Phys.* **1979**, *17*, 851.
(29) Kirst, K. U.; Kremer, F.; Pakula, T.; Hollingshurst, J. *Colloid Polym. Sci.* **1994**, *272*, 1420.
(30) Kirst, K. U.; Kremer, F.; Litvinov, V. M. *Macromolecules* **1993**, *26*, 975.
(31) Alegria, A.; Gomez, D.; Colmenero, J. *Macromolecules* **2002**, *35*, 2030.
(32) Boersma, A.; van Turnhout, J.; Wubbenhorst, M. *Macromolecules* **1998**, *31*, 7453. Diaz-Calleja, R. *Macromolecules* **2000**, *33*, 8924.
(33) Goodwin, A. A.; Beevers, M. S.; Clarson, S. J.; Semlyen, J. A. *Polymer* **1996**, *37*, 2603.
(34) Marks, J. E. *Physical Properties of Polymers Handbook*; American Institute of Physics: New York, 1996.
(35) Schick, C.; Wurm, A.; Mohammed, A. *Polymer Crystallization: Observations, Concepts and Interpretations*; Springer-Verlag: Berlin, Germany, 2003.
(36) Lorthioir, C.; Alegria, A.; Colmenero, J. Manuscript in preparation.
(37) Cendoya, I.; Alegria, A.; Alberdi, J. M.; Colmenero, J.; Grimm, H.; Richter, D.; Frick, B. *Macromolecules* **1999**, *32*, 4065. Zetsche, A.; Fischer, E. W. *Acta Polym.* **1994**, *45*, 168.
(38) Prevosto, D.; Lucchesi, M.; Capaccioli, S.; Casalini, R.; Rolla, P. A. *Phys. Rev. B* **2003**, *67*, 174202.

MA049011T